

198532: semipelitic gneiss, Brunswick River

(*South West Terrane, Yilgarn Craton*)

Blereau, ER, Korhonen, FJ, Fielding, IOH, Romano, SS, Kelsey, DE and Roberts, MP

Location and sampling

COLLIE (SI 50-6), BUNBURY (2031)

MGA Zone 50, 695881E 6321871N

Warox Site SXWBGD198532

Sampled on 3 June 2010

This sample was collected from an outcrop on a sharp bend on Clifton Road, on the south side of the Brunswick River, about 4.5 km east-northeast of Brunswick Junction (4.9 km along Clifton Road from the South Western Highway), 3.0 km west of the Beela railway stop and 0.6 km northwest of the intersection of Clifton and Alcock Roads. The sample was collected as part of the Yilgarn Craton Metamorphic Project (2003–14) undertaken by Ben Goscombe for the Geological Survey of Western Australia (GSWA), and referred to in that study as sample BG10-16. The results from this project have not been released by GSWA, although select data have been published in Goscombe et al. (2019).

Geological context

The unit sampled is a semipelitic gneiss at the western margin of the South West Terrane of the Yilgarn Craton, within a north-trending belt of Archean metasedimentary and gneissic rocks by Wilde (2001) as the informally named Balingup Terrane. This terrane contains some of the youngest granitic rocks in the Yilgarn Craton, with U–Pb zircon dates of 2.61 – 2.53 Ga (e.g. Wilde et al., 1996). The sample locality is about 3.8 km east of the Darling Fault, which is >1000 km long and forms the boundary between Precambrian rocks of the Yilgarn Craton and Paleozoic and younger rocks of the Perth Basin. The Darling Fault may have been initiated during the Archean (Blight et al., 1981), and was active during the Proterozoic and Phanerozoic, and possibly into the Neogene (Thomas, 2014). SHRIMP zircon geochronology of the sample reported here yielded U–Pb ages of 3296–1402 Ma for detrital zircons, a conservative maximum depositional age of 1654 ± 35 Ma, a poorly constrained metamorphic component at 898–751 Ma, and a younger metamorphic age of 707 ± 5 Ma (GSWA 198532, Wingate et al., 2014).

Petrographic description

The sample is a medium- to very fine-grained, strongly foliated, pelitic gneiss, consisting of about 62% quartz, 19% muscovite and sericite, 7% garnet, 5% biotite, 4% chlorite, 1–2% plagioclase, and trace amounts of magnetite, ilmenite and zircon (Fig. 1; Table 1). Much of this sample consists of a medium-grained quartzose intergrowth composed of elongated, strained quartz grains from 0.1 to 4 mm across, arranged with most long axes parallel to the foliation. Muscovite occurs mostly as sericite and occurs as extremely fine-grained matted aggregates up to 2 mm wide, sheared into augen shapes and layers that wrap around garnet porphyroblasts, defining the foliation (Figs 1, 2). Coarser muscovite grains up to 0.2 mm in size also occur with biotite (Fig. 2b). Equant anhedral garnet porphyroblasts are cracked and up to 4 mm in size, with cores rich in rounded quartz inclusions and rims free of inclusions (Figs 1, 2). Garnet porphyroblasts are almandine-rich ($X_{\text{Alm}} = 0.71$, $X_{\text{Prp}} = 0.21$, $X_{\text{Grs}} = 0.06$, $X_{\text{Sps}} = 0.02$) with weak compositional zoning along cracks and the most outer rims (Appendix 1). Biotite in the matrix partly defines the foliation and ranges in size from 0.5 to 2 mm, with variable chloritization (Fig. 2a). Chlorite forms fine-grained matted aggregates that replace garnet and biotite along fractures or at their edges, and also within muscovite–sericite lenses. Anhedral grains of plagioclase are up to 2.5 mm in diameter and show partial replacement to sericite. This amphibolite facies gneiss was likely derived from a semipelitic, quartz-rich metasedimentary protolith.

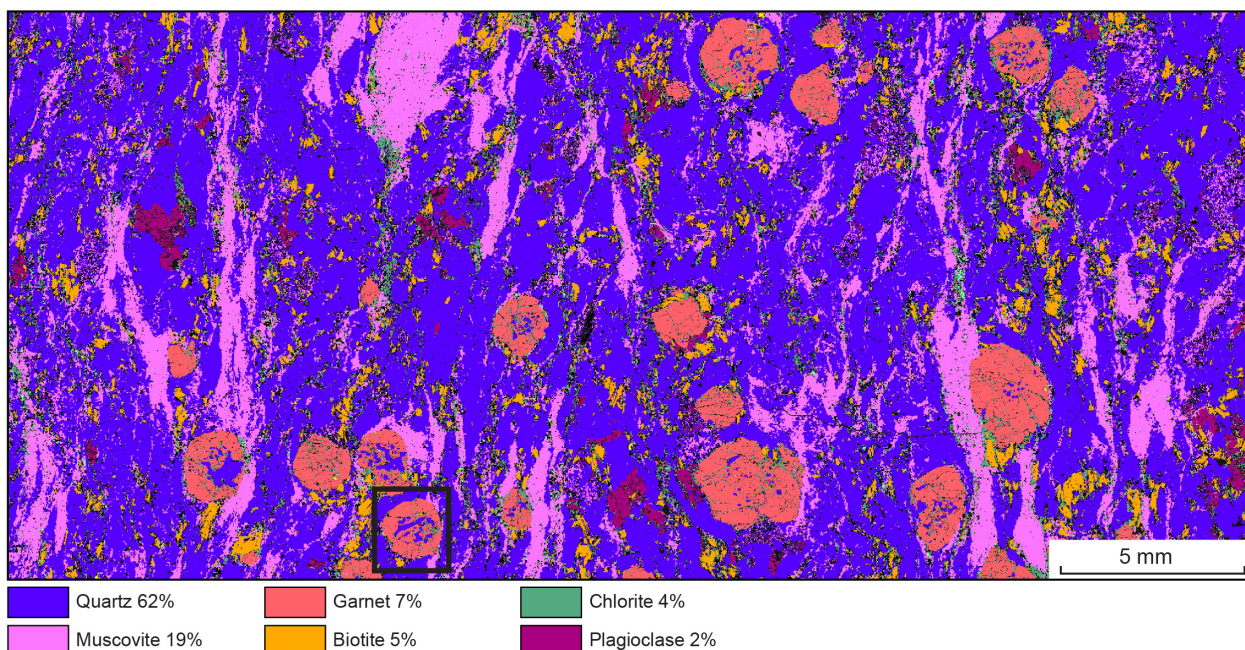


Figure 1. TESCAN Integrated Mineral Analyser (TIMA) image of an entire thin section from sample 198532: semipelitic gneiss, Brunswick River. Volume percent proportions of major rock-forming minerals are calculated by the TIMA software. Black rectangle shows location of electron probe microanalyser (EPMA) garnet map (Appendix 1)

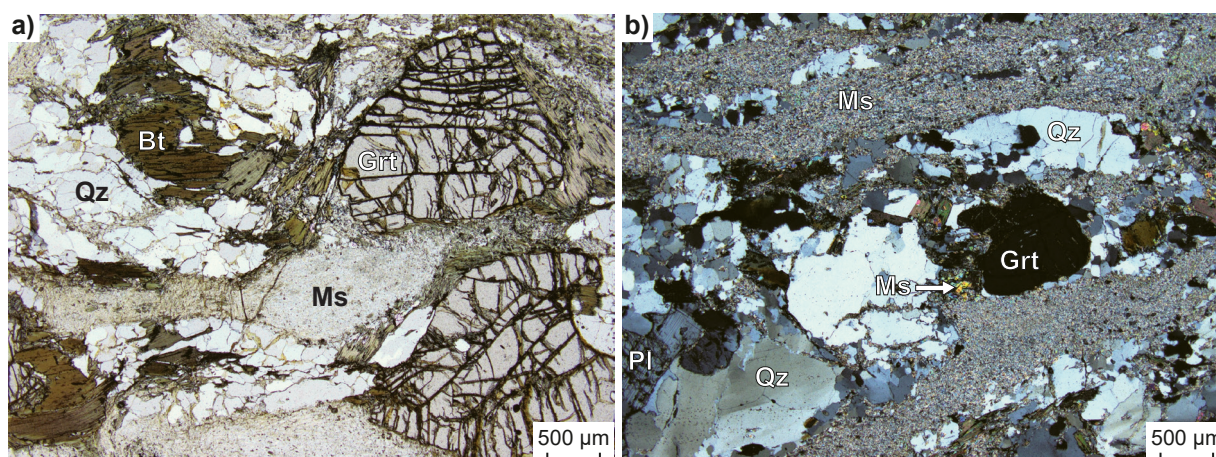


Figure 2. Photomicrographs of sample 198532: semipelitic gneiss, Brunswick River: a) plane-polarized light; b) crossed polarized light. Mineral abbreviations are explained in the caption to Figure 3

Table 1. Mineral modes for sample 198532: semipelitic gneiss, Brunswick River

Mineral modes	Grt	Sil	Ms	Bt	Pl	Qz	Ilm	Mag	H ₂ O
Observed (vol%) ^(a)	7	–	19	5	2	62	trace	trace	–
Predicted (mol%)									
@ 890 °C, 4.1 kbar	trace	9	8	19	2	59	1	0.4	3
@ 890 °C, 6.2 kbar	1	8	11	17	1	58	1	0.4	3

NOTES: (a) Muscovite occurs with sericite, and up to 4% chlorite also present in thin section
– not present

Analytical details

Preliminary P – T estimates were obtained using multiple-reaction thermobarometry calculated from the mineral compositions (Table 2; Goscombe et al., 2015). These estimates were derived from the ‘averagePT’ module (avPT) in the program THERMOCALC version tc325 (Powell and Holland, 1988), using the internally consistent Holland and Powell (1998) dataset.

The metamorphic evolution of this sample was investigated using phase equilibria modelling, based on the bulk-rock composition (Table 3). The bulk-rock composition was determined by X-ray fluorescence spectroscopy, together with loss on ignition (LOI). FeO content was analysed by Fe²⁺ titration, and Fe₂O₃ calculated by difference. The modelled O content (for Fe³⁺) was derived from the titration value; the modelled H₂O content was the measured LOI. The bulk composition was adjusted for the presence of apatite by applying a correction to CaO (Table 3). Thermodynamic calculations were performed in the MnNCKFMASHTO (MnO–Na₂O–CaO–K₂O–FeO–MgO–Al₂O₃–SiO₂–H₂O–TiO₂–O) system using THERMOCALC version tc340 (Powell and Holland 1988; updated October 2013) and the internally consistent thermodynamic dataset of Holland and Powell (2011; dataset tc-ds62, created in February 2012). The activity–composition relations used in the modelling are detailed in White et al. (2014a,b). Additional information on the workflow with relevant background and methodology are provided in Korhonen et al. (2020).

Table 2. Mineral compositions for sample 198532: semipelitic gneiss, Brunswick River

Mineral ^(a)	Grt	Grt	Grt	Grt	Bt	Bt	Pl	Pl	Ms	Grt
Setting ^(b)	Core	Mantle	Rim	OR	Core	Rim	Core	Rim	Core	OR
<i>wt%</i>										
SiO ₂	38.11	37.72	38.16	38.33	35.86	36.24	60.61	60.99	46.42	37.74
TiO ₂	0.00	0.02	0.02	0.01	1.58	1.55	0.00	0.00	0.09	0.00
Al ₂ O ₃	21.46	21.07	21.39	21.62	18.82	18.70	24.86	25.10	35.33	21.58
Cr ₂ O ₃	0.05	0.02	0.00	0.04	0.00	0.03	0.00	0.00	0.00	0.00
FeO	32.97	33.08	34.40	34.71	20.31	20.17	0.04	0.00	1.68	30.97
MnO	0.93	1.11	1.46	1.55	0.06	0.00	0.00	0.00	0.00	1.03
MgO	5.13	4.92	4.03	3.82	9.91	9.93	0.00	0.00	0.84	7.42
ZnO	0.04	0.05	0.00	0.00	0.14	0.06	0.00	0.00	0.05	0.00
CaO	1.75	1.96	1.82	1.80	0.01	0.01	6.90	6.70	0.00	1.33
Na ₂ O	0.04	0.01	0.01	0.03	0.24	0.19	8.06	8.06	0.55	0.00
K ₂ O	0.04	0.00	0.00	0.01	9.24	9.32	0.11	0.06	10.01	0.02
Total ^(c)	100.53	99.97	101.28	101.92	96.15	96.22	100.59	100.91	94.96	100.09
Oxygen	12	12	12	12	11	11	8	8	11	12
Si	3.00	3.00	3.01	3.01	2.71	2.73	2.68	2.69	3.11	2.95
Ti	0.00	0.00	0.00	0.00	0.09	0.09	0.00	0.00	0.00	0.00
Al	1.99	1.97	1.99	2.00	1.67	1.66	1.30	1.30	2.78	1.99
Cr	0.00	0.00	0.00	0.00	0.00	0.00	0.00	0.00	0.00	0.00
Fe ^{3+(d)}	0.00	0.03	0.00	0.00	0.06	0.06	0.00	0.00	0.00	0.12
Fe ²⁺	2.17	2.17	2.27	2.28	1.22	1.21	0.00	0.00	0.09	1.90
Mn ²⁺	0.06	0.07	0.10	0.10	0.00	0.00	0.00	0.00	0.00	0.07
Mg	0.60	0.58	0.47	0.45	1.11	1.11	0.00	0.00	0.08	0.86
Zn	0.00	0.00	0.00	0.00	0.01	0.00	0.00	0.00	0.00	0.00
Ca	0.15	0.17	0.15	0.15	0.00	0.00	0.33	0.32	0.00	0.11
Na	0.01	0.00	0.00	0.00	0.03	0.03	0.69	0.69	0.07	0.00
K	0.00	0.00	0.00	0.00	0.89	0.89	0.01	0.00	0.85	0.00
Total	8.00	8.00	8.00	8.00	7.80	7.78	5.00	5.00	7.00	8.00
<i>Compositional variables</i>										
XFe ^(e)	0.78	0.79	0.83	0.84	0.52	0.52	–	–	0.53	0.69

NOTES:

–, not applicable

(a) Mineral abbreviations explained in the caption to Figure 2

(b) OR, outer rim

(c) Totals on anhydrous basis

(d) Fe³⁺ contents for biotite assumed to be 10% of Fe total; Fe³⁺ contents for other minerals based on Droop (1987)

(e) XFe = Fe²⁺/(Fe²⁺ + Mg)

<i>XRF whole-rock composition (wt%)^(a)</i>												
SiO₂	TiO₂	Al₂O₃	Fe₂O₃^(b)	FeO^(b)	MnO	MgO	CaO	Na₂O	K₂O	P₂O₅	LOI	Total
72.91	0.64	12.42	1.90	4.59	0.09	1.89	0.21	0.19	2.82	0.04	1.90	99.60
<i>Normalized composition used for phase equilibria modelling (mol%)</i>												
SiO₂	TiO₂	Al₂O₃	O^(c)	FeO^{T(d)}	MnO	MgO	CaO^(e)	Na₂O	K₂O	–	H₂O^(f)	Total
73.83	0.49	7.41	0.72	5.33	0.79	2.85	0.16	0.19	1.82	–	6.41	100

Results

Metamorphic P – T estimates have been derived based on detailed examination of one thin section and the bulk-rock composition; care was taken to ensure that the thin section and the sample volume selected for whole-rock chemistry were similar in terms of featuring the same minerals in approximately the same abundances (Table 1), to minimize any potential compositional differences. The P – T pseudosection for sample 198532 was calculated over a P – T range of 3–8 kbar and 570–750 °C (Fig. 3). The H_2O -saturated solidus is located between 670 and 695 °C across the range of modelled pressures. Chlorite is stable at the lowest temperatures across the range of modelled pressures, followed by epidote, staurolite and sillimanite with increasing temperature. Aluminosilicate minerals, mainly sillimanite, have a broad stability over most of the modelled conditions. Magnetite is stable below 665 °C at 3 kbar and 7.4 kbar at 750 °C. Cordierite is stable at temperatures above 675 °C and pressures below 5 kbar. Garnet is stable above 3.5 kbar at 570 °C and above 4 kbar at 720 °C.

Metamorphic P - T estimates ($\pm 2\sigma$ uncertainty) calculated using multiple-reaction thermobarometry are 6.4 ± 0.98 kbar and 588 ± 27 °C (Goscombe et al., 2015). These calculations used the core compositions (Table 2) to estimate peak conditions.

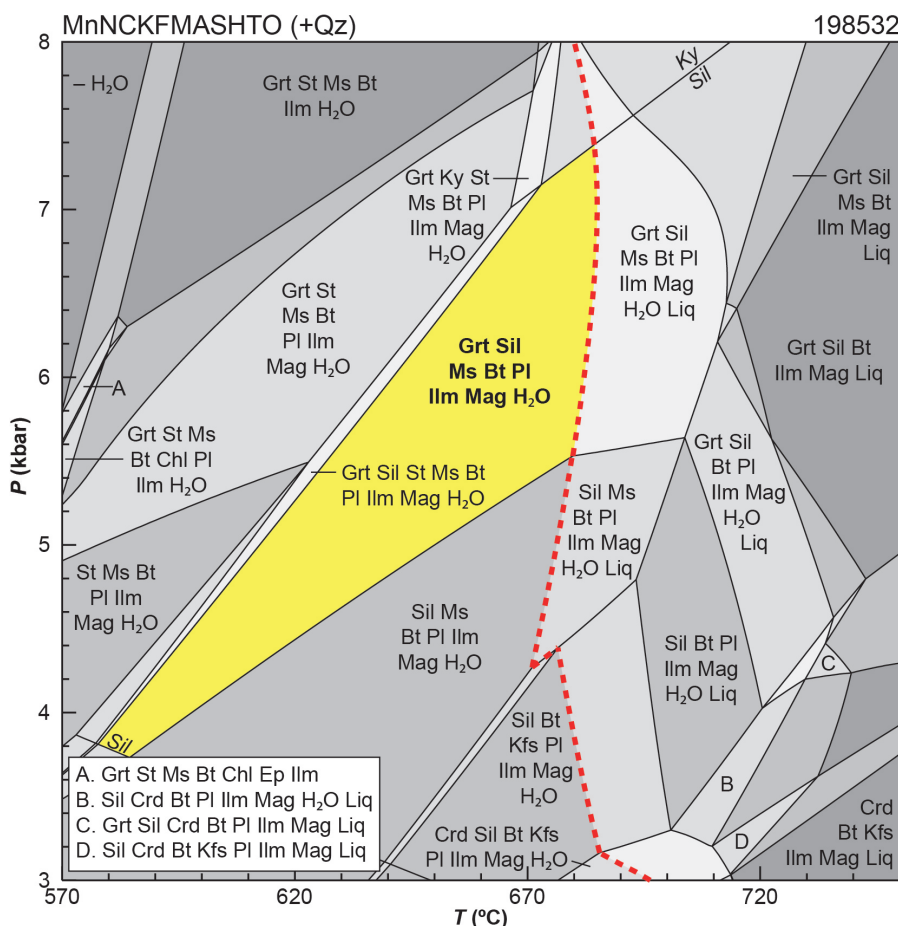


Figure 3. *P-T* pseudosection calculated for 198532: semipelitic gneiss, Brunswick River. Assemblage field corresponding to peak metamorphic conditions are delimited by bold text and yellow shading. Red dashed line represents the solidus. Abbreviations: Bt, biotite; Chl, chlorite; Crd, cordierite; Ep, epidote; Grt, garnet; H₂O, fluid (pure H₂O); Ilm, ilmenite; Kfs, K-feldspar; Ky, kyanite; Liq, silicate melt; Mag, magnetite; Ms, muscovite; Pl, plagioclase; Qz, quartz; Sil, sillimanite; St, staurolite

Interpretation

The preserved mineral assemblage is garnet–muscovite–biotite–plagioclase–quartz–ilmenite–magnetite. There is no evidence in the thin section for partial melting. The modelling predicts that garnet-bearing assemblages below the solidus also include staurolite at lower temperatures, followed by the loss of staurolite and the growth of sillimanite at progressively higher temperatures. Neither staurolite nor sillimanite are observed in the sample; however, sillimanite is susceptible to retrogression, particularly during shearing and hydration. The sample is strongly deformed and hydrated, and zircon dates indicate multiple metamorphic events. Based on this complicated history, sillimanite is inferred to have been part of the peak metamorphic assemblage, but was completely retrogressed to muscovite during fluid-present deformation.

The inferred peak assemblage of garnet–sillimanite–muscovite–biotite–plagioclase–quartz–ilmenite–magnetite–H₂O has a broad stability between 580 and 685 °C at 3.7 – 7.4 kbar. Results calculated from multiple-reaction thermobarometry are broadly consistent with equilibration in this field. Up to 9 mol% (equivalent to vol%) sillimanite is predicted in this field, which is interpreted to have been retrogressed to muscovite. The peak field is delimited by the loss of garnet at lower pressure, kyanite at higher pressure, staurolite at lower temperature, and partial melting at higher temperatures. The predicted modes of quartz, plagioclase and the Fe–Ti oxides within the peak field at 660 °C are similar to the modes observed in the thin section (Table 1). The observed mode of muscovite (= 19%) accounts for the amount of predicted muscovite (8–11%) and the retrogression of peak sillimanite (8–9%; Table 1). However, the predicted modes of garnet and biotite are lower than observed values, although this discrepancy may be due to variations between the material used for whole-rock chemistry and the thin section.

Peak metamorphic conditions are estimated at 580–685 °C and 3.7 – 7.4 kbar, with an apparent thermal gradient between 90 and 155 °C/kbar. With the exception of extensive sericite alteration throughout the sample, there is no information on the post-peak history or the overall P–T trajectory preserved in the sample.

References

- Blight, DF, Compston, W and Wilde, SA 1981, The Logue Brook Granite, in Annual report for the year 1980: Geological Survey of Western Australia, p. 72–80.
- Droop, GTR 1987, A general equation for estimating Fe³⁺ concentrations in ferromagnesian silicates and oxides from microprobe analyses, using stoichiometric criteria: *Mineralogical Magazine*, v. 51, no. 361, p. 431–435.
- Goscombe, B, Blewett, R, Groenewald, PB, Foster, D, Wade, B, Wyche, S, Wingate, MTD and Kirkland, CL 2015, Metamorphic Evolution of the Yilgarn Craton: Geological Survey of Western Australia, 910p., (unpublished).
- Goscombe, B, Foster, DA, Blewett, R, Czarnota, K, Wade, B, Groenewald, B and Gray, D 2019, Neoproterozoic metamorphic evolution of the Yilgarn Craton: a record of subduction, accretion, extension and lithospheric delamination: *Precambrian Research*, article no. 105441, doi:10.1016/j.precamres.2019.105441.
- Holland, TJB and Powell, R 2011, An improved and extended internally consistent thermodynamic dataset for phases of petrological interest, involving a new equation of state for solids: *Journal of Metamorphic Geology*, v. 29, no. 3, p. 333–383.
- Korhonen, FJ, Kelsey, DE, Fielding, IOH and Romano, SS 2020, The utility of the metamorphic rock record: constraining the pressure–temperature–time conditions of metamorphism: Geological Survey of Western Australia, Record 2020/14, 24p.
- Powell, R and Holland, TJB 1988, An internally consistent dataset with uncertainties and correlations: 3. Applications to geobarometry, worked examples and a computer program: *Journal of Metamorphic Geology*, v. 6, no. 2, p. 173–204.
- Thomas, CM 2014, The tectonic framework of the Perth Basin: current understanding: Geological Survey of Western Australia, Record 2014/14, 36p.
- White, RW, Powell, R, Holland, TJB, Johnson, TE and Green, ECR 2014a, New mineral activity–composition relations for thermodynamic calculations in metapelitic systems: *Journal of Metamorphic Geology*, v. 32, no. 3, p. 261–286.
- White, RW, Powell, R and Johnson, TE 2014b, The effect of Mn on mineral stability in metapelites revisited: New a–x relations for manganese-bearing minerals: *Journal of Metamorphic Geology*, doi:10.1111/jmg.12095.
- Wilde, SA 2001, Jamperding and Chittering metamorphic belts, Western Australia — a field guide: Geological Survey of Western Australia, Record 2001/12, 24p.
- Wilde, SA, Middleton, MF and Evans, BJ 1996, Terrane accretion in the southwestern Yilgarn Craton: Evidence from a deep seismic crustal profile: *Precambrian Research*, v. 78, p. 179–196.
- Wingate, MTD, Kirkland, CL, Goscombe, B and Wyche, S 2014, 198532: pelitic gneiss, Brunswick River; Geochronology Record 1214: Geological Survey of Western Australia, 7p.

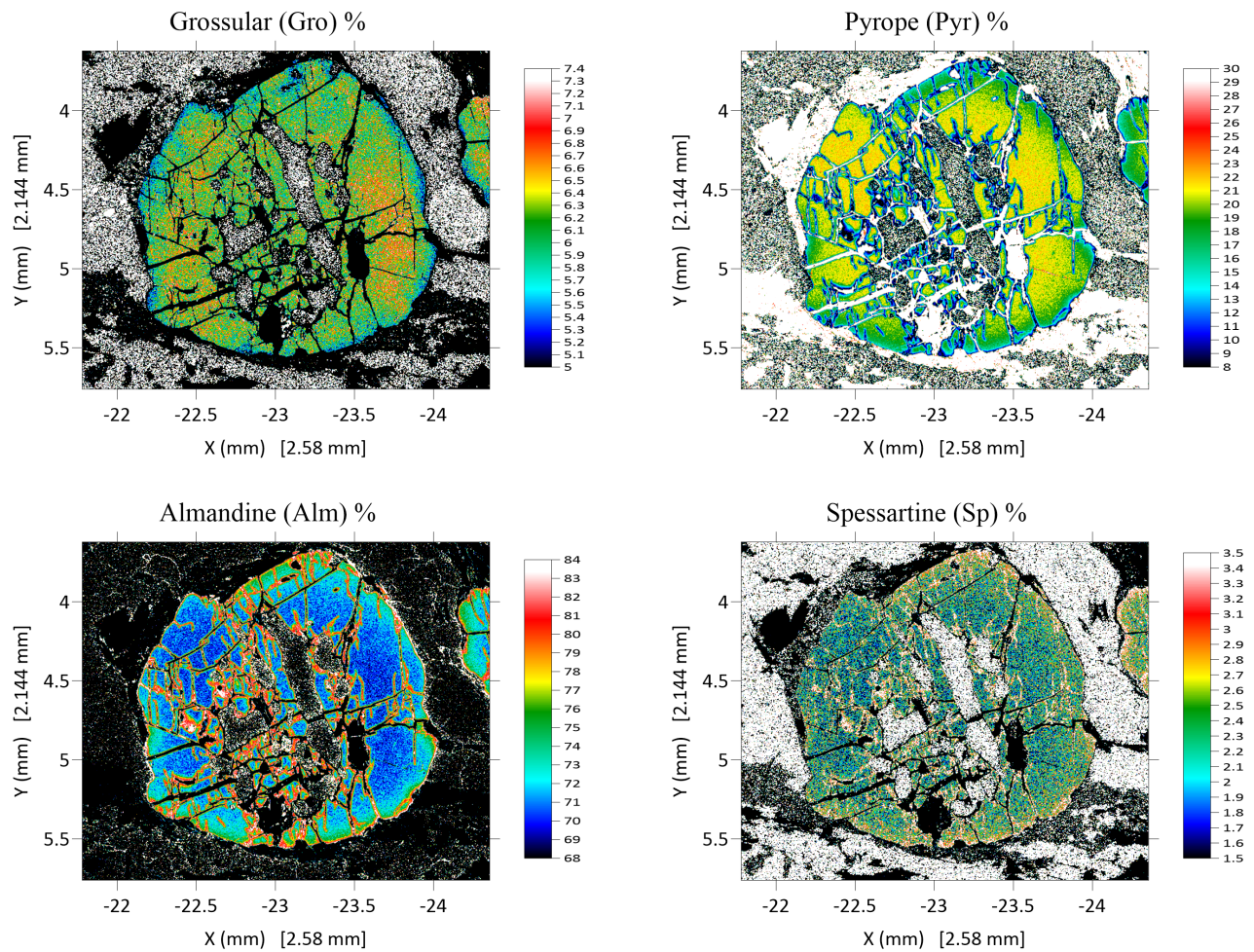
Links

Metamorphic history introduction document: [Intro_2020.pdf](#)

Appendix

Quantitative EPMA compositional maps for sample 198532: semipelitic gneiss, Brunswick River, calculated for proportion of garnet end-members. The analysed garnet grain is identified in Figure 1

198532



Recommended reference for this publication

Blereau, ER, Korhonen, FJ, Fielding, IOH, Romano, SS, Kelsey DE and Roberts MP 2021, 198532: semipelitic gneiss, Brunswick River; Metamorphic History Record 2: Geological Survey of Western Australia, 7p.

Data obtained: 10 September 2020

Date released: 25 June 2021

This Metamorphic History Record was last modified on 9 June 2021.

Grid references in this publication refer to the Geocentric Datum of Australia 1994 (GDA94). All locations are quoted to at least the nearest 100 m.

WAROX is GSWA's field observation and sample database. WAROX site IDs have the format 'ABCXXXnnnnnnSS', where ABC = geologist username, XXX = project or map code, nnnnnn = 6 digit site number, and SS = optional alphabetic suffix (maximum 2 characters).

Isotope and element analyses are routinely conducted using the GeoHistory laser ablation ICP-MS and Sensitive High-Resolution Ion Microprobe (SHRIMP) ion microprobe facilities at the John de Laeter Centre (JdLC), Curtin University, with the financial support of the Australian Research Council and AuScope National Collaborative Research Infrastructure Strategy (NCRIS). The TESCAN Integrated Mineral Analyser (TIMA) instrument was funded by a grant from the Australian Research Council (LE140100150) and is operated by the JdLC with the support of the Geological Survey of Western Australia, The University of Western Australia (UWA) and Murdoch University. Mineral analyses are routinely obtained using the electron probe microanalyser (EPMA) facilities at the Centre for Microscopy, Characterisation and Analysis at UWA, and at Adelaide Microscopy, University of Adelaide.

Digital data related to WA Geology Online, including geochronology and digital geology, are available online at the Department's [Data and Software Centre](#) and may be viewed in map context at [GeoVIEW.WA](#).

Disclaimer

This product uses information from various sources. The Department of Mines, Industry Regulation and Safety (DMIRS) and the State cannot guarantee the accuracy, currency or completeness of the information. Neither the department nor the State of Western Australia nor any employee or agent of the department shall be responsible or liable for any loss, damage or injury arising from the use of or reliance on any information, data or advice (including incomplete, out of date, incorrect, inaccurate or misleading information, data or advice) expressed or implied in, or coming from, this publication or incorporated into it by reference, by any person whosoever.



© State of Western Australia (Department of Mines, Industry Regulation and Safety) 2021

With the exception of the Western Australian Coat of Arms and other logos, and where otherwise noted, these data are provided under a Creative Commons Attribution 4.0 International Licence. (<http://creativecommons.org/licenses/by/4.0/legalcode>)

Further details of geoscience products are available from:

Information Centre
Department of Mines, Industry Regulation and Safety
100 Plain Street
EAST PERTH WA 6004
Telephone: +61 8 9222 3459 | Email: publications@dmirs.wa.gov.au
www.dmirs.wa.gov.au/GSWApublications